


BRAIN COMMUNICATIONS

Hypokalaemic periodic paralysis with a charge-retaining substitution in the voltage sensor

Tomoya Kubota,^{1,2,3} Fenfen Wu,⁴ Savine Vicart,⁵ Maki Nakaza,¹ Damien Sternberg,⁵ Daisuke Watanabe,⁶ Mitsuru Furuta,^{2,7} Yosuke Kokunai,^{2,5} Tatsuya Abe,⁶ Norito Kokubun,⁸ Bertrand Fontaine,^{5,*} Stephen C. Cannon^{4,*} and  Masanori P. Takahashi^{1,2,*}

Familial hypokalaemic periodic paralysis is a rare skeletal muscle disease caused by the dysregulation of sarcolemmal excitability. Hypokalaemic periodic paralysis is characterized by repeated episodes of paralytic attacks with hypokalaemia, and several variants in *CACNA1S* coding for Cav1.1 and *SCN4A* coding for Nav1.4 have been established as causative mutations. Most of the mutations are substitutions to a non-charged residue, from the positively charged arginine (R) in transmembrane segment 4 (S4) of a voltage sensor in either Cav1.1 or Nav1.4. Mutant channels have aberrant leak currents called 'gating pore currents', and the widely accepted consensus is that this current is the essential pathological mechanism that produces susceptibility to anomalous depolarization and failure of muscle excitability during a paralytic attack. Here, we have identified five hypokalaemic periodic paralysis cases from two different ethnic backgrounds, Japanese and French, with charge-preserving substitutions in S4 from arginine, R, to lysine, K. An R to K substitution has not previously been reported for any other hypokalaemic periodic paralysis families. One case is R219K in Nav1.4, which is located at the first charge in S4 of Domain I. The other four cases all have R897K in Cav1.1, which is located at the first charge in S4 of Domain III. Gating pore currents were not detected in expression studies of Cav1.1-R897K. Nav1.4-R219K mutant channels revealed a distinct, but small, gating pore current. Simulation studies indicated that the small-amplitude gating pore current conducted by Nav1.4-R219K is not likely to be sufficient to be a risk factor for depolarization-induced paralytic attacks. Our rare cases with typical hypokalaemic periodic paralysis phenotypes do not fit the canonical view that the essential defect in hypokalaemic periodic paralysis mutant channels is the gating pore current and raise the possibility that hypokalaemic periodic paralysis pathogenesis might be heterogeneous and diverse.

- 1 Division of Health Sciences, Department of Functional Diagnostic Science, Osaka University Graduate School of Medicine, 1-7, Yamadaoka, Suita, Osaka, 5650871, Japan
- 2 Department of Neurology, Osaka University Graduate School of Medicine, Suita, Osaka, Japan
- 3 Department of Biochemistry and Molecular Biology, The University of Chicago, Chicago, IL 60637, USA
- 4 Department of Physiology, David Geffen School of Medicine, University of California, Los Angeles, Los Angeles, CA, USA
- 5 Sorbonne Université, INSERM, Assistance Publique -Hôpitaux de Paris, Center of Research in Myology-UMR 974, Service of Neuro-Myology (CMR Muscle Channelopathies), Institute of Myology, University Hospital Pitié-Salpêtrière, Paris, France
- 6 Department of Neurology, National Hospital Organization Hakone Hospital, Odawara, Japan
- 7 Department of Neurology, Kansai Rosai Hospital, Amagasaki, Hyogo, Japan
- 8 Department of Neurology, Dokkyo Medical University, Tochigi, Japan

Correspondence to: Masanori P. Takahashi, Division of Health Sciences, Department of Functional Diagnostic Science, Osaka University Graduate School of Medicine, 1-7, Yamadaoka, Suita, Osaka 5650871, Japan
E-mail: mtakahas@neurol.med.osaka-u.ac.jp

Received May 26, 2020. Revised May 26, 2020. Accepted June 2, 2020. Advance Access publication July 16, 2020

© The Author(s) (2020). Published by Oxford University Press on behalf of the Guarantors of Brain.

This is an Open Access article distributed under the terms of the Creative Commons Attribution Non-Commercial License (<http://creativecommons.org/licenses/by-nc/4.0/>), which permits non-commercial re-use, distribution, and reproduction in any medium, provided the original work is properly cited. For commercial re-use, please contact journals.permissions@oup.com

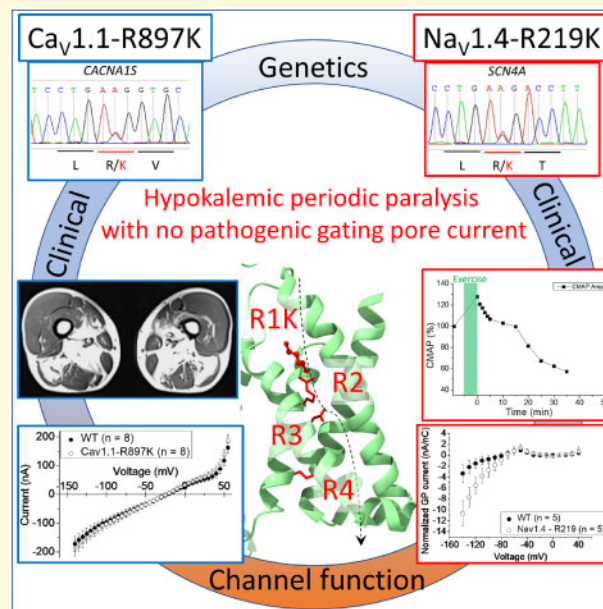
Correspondence may also be addressed to: Stephen C. Cannon, Department of Physiology, David Geffen School of Medicine at UCLA, Los Angeles, CA 90095-1751, USA
E-mail: sccannon@mednet.ucla.edu

Correspondence may also be addressed to: Bertrand Fontaine, Sorbonne Université, INSERM Assistance Publique -Hôpitaux de Paris, Center of Research in Myology-UMR 974, Service of Neuro-Myology (CMR Muscle Channelopathies), Institute of Myology, University Hospital Pitié-Salpêtrière, F-75013, Paris, France
E-mail: bertrand.fontaine@upmc.fr

Keywords: hypokalaemic periodic paralysis; voltage sensing domain; Na_v ; Ca_v ; gating pore current

Abbreviations: CMAP=compound muscle action potential; HypoPP=hypokalaemic periodic paralysis; MRC=Medical Research Council; VSD=voltage sensor domain.

Graphical Abstract



Introduction

Familial hypokalaemic periodic paralysis (HypoPP) is a rare skeletal muscle disease caused by the dysregulation of sarcolemmal excitability (Cannon, 2015). HypoPP is characterized by repeated episodes of weakness in the setting of hypokalaemia, and several mutations in *CACNA1S* encoding $\text{Ca}_v1.1$ and *SCN4A* encoding $\text{Na}_v1.4$, have been identified as causative (Venance *et al.*, 2006). Most mutations are substitutions of a positively charged arginine (R) in the fourth transmembrane segment (S4) within a voltage sensor domain (VSD) of either $\text{Ca}_v1.1$ or $\text{Na}_v1.4$ (Cannon, 2010). The reason why mutations in two different channels can cause identical clinical manifestations had been a mystery for a long time. The explanation came when the biophysical experiments using Shaker K^+ channel and voltage-gated Na^+ channels demonstrated that missense mutations of arginine residues in the S4 segments create a leakage current, called the ‘omega current’ or ‘gating pore current’ (Starace and

Bezanilla, 2004; Sokolov *et al.*, 2007). Subsequently, similar leak currents were detected in muscle fibres isolated from HypoPP mouse models with $\text{Ca}_v1.1\text{-R528H}$ and $\text{Na}_v1.4\text{-R663H}$, S4 arginine to histidine knock-in mutations (Wu *et al.*, 2011, 2012). Computational models of fibre excitability show that although the gating pore leak is small (about 5% of the total resting conductance of the fibre), the current is sufficient to cause paradoxical depolarization of the resting potential in low extracellular K^+ , which is the hallmark of HypoPP. This ‘gating pore current theory’ has been postulated to be the common pathogenic feature in HypoPP (Matthews *et al.*, 2009; Cannon, 2010). Interestingly, a mutation of the $\alpha 2$ subunit of the $\text{Na}^+/\text{K}^+\text{-ATPase}$ encoded by *ATP1A2* has been recently reported to be responsible for HypoPP by producing anomalous leak current, which further strengthens the unifying pathomechanism (Sampedro Castañeda *et al.*, 2018).

For 19 of 20 reported HypoPP mutations, the genetic lesion causes substitution of arginine to a non-charged

residue in the S4 segment of a VSD. Functional expression studies have demonstrated gating pore currents in all 11 HypoPP R/X mutations in S4 segments of $\text{Na}_v1.4$ channels (Sokolov *et al.*, 2007; Struyk and Cannon, 2007; Struyk *et al.*, 2008; Francis *et al.*, 2011; Bayless-Edwards *et al.*, 2018) and all 4 of the S4 R/X mutants tested in $\text{Ca}_v1.1$ (Wu *et al.*, 2012, 2018b; Fuster *et al.*, 2017a). For the one exception, p. Val876Glu in the S3 segment of domain III in $\text{Ca}_v1.1$, expression studies also detected a gating pore current (Fuster *et al.*, 2017a). All available data are consistent with the notion that the gating pore current, usually as the result of a non-charged R/X missense mutation in the S4 segment of a VSD, is the essential anomaly that produces susceptibility to episodic loss of fibre excitability during attacks of weakness in HypoPP. Moreover, from the biophysical point of view on the structure–function relations for the VSDs in $\text{Na}_v1.4$ or $\text{Ca}_v1.1$, it is plausible that the loss of a positively charged residue might be necessary for the generation of gating pore currents, by disrupting the interactions with the counter negatively charged residues, glutamate (E) or aspartate (D), in S2 and S3 (Tao *et al.*, 2010; Pan *et al.*, 2018).

Here, we report that five patients with typical HypoPP clinical phenotypes from four pedigrees (two Japanese and two French), harbouring missense from arginine to lysine (R/K) mutations, which preserves the positive charge in the voltage sensor in either $\text{Na}_v1.4$ or $\text{Ca}_v1.1$. We detected a gating pore current for the R219K mutation in $\text{Na}_v1.4$, albeit with a very small amplitude that was about 1/17th of that seen for other non-charge preserving R/X HypoPP mutations. Conversely, we were unable to detect a gating pore current for the R897K mutation in $\text{Ca}_v1.1$. Our results suggest that alternative mechanisms, besides the canonical gating pore current, may also be a cause of intermittent loss of fibre excitability in HypoPP.

Materials and methods

Patient consent and genetic analysis

We reported clinical information of Japanese patients under the approval of the ethical committee in Osaka university medical hospital. We conducted the genetic analysis after obtaining written form of the informed consent which has been approved by the ethical committee in Osaka university graduate school of medicine. Genetic diagnosis in French patients was performed in accordance with French Bioethics Laws.

Genomic DNA was extracted from the patients' blood lymphocytes. The region comprising all exons of *SCN4A*, *CACNA1S* and *KCNJ2* gene were amplified by PCR, and the purified fragments were sequenced using an automated DNA sequencer (Big Dye Terminator v 3.1 and ABI310; PE Applied Biosystems, Foster City, CA, USA).

Molecular biology

The α and $\beta 1$ subunits of the rat skeletal muscle voltage-gated sodium channel ($\text{rNa}_v1.4$) were cloned into pBSTA vectors for expression studies in *Xenopus* oocytes. For patch-clamp experiments using HEK293t cells, the human skeletal muscle $\text{Na}_v1.4$ channel ($\text{hNa}_v1.4$) and $\beta 1$ subunit were cloned into the mammalian expression construct, pRc/CMV. The R291K missense mutation of $\text{Na}_v1.4$ was introduced with the site-directed mutagenesis kit (KOD-Plus mutagenesis kit; TOYOBO, Osaka, Japan) and verified by Sanger sequencing.

The human α_{1S} subunit of the calcium channel ($\text{hCa}_v1.1$) was co-expressed with rat $\alpha_2\delta$, rabbit β_1 and mouse Stac3, as previously described (Wu *et al.*, 2018b). The $\text{Ca}_v1.1$, Stac3 and β_1 constructs were subcloned into an oocyte-optimized expression vector, pGEMHE (Liman *et al.*, 1992) and the $\alpha_2\delta$ cDNA was subcloned into pcDNA3. Site-directed mutagenesis of $\text{Ca}_v1.1$ to create $\text{Ca}_v1.1$ -R897K was performed with the QuikChange II mutagenesis kit (Agilent) and verified by sequencing the entire cDNA insert and flanking regions of pGEMHE.

Expression of $\text{rNa}_v1.4$, $\text{rNa}_v\beta 1$ and $\text{hCa}_v1.1$ in *Xenopus* oocytes

For expression studies of $\text{rNa}_v1.4$ in oocytes, cRNAs for the α and $\beta 1$ subunits were transcribed *in vitro* using the T7 mMESSAGE cRNA kit (Ambion). Freshly isolated oocytes from *Xenopus laevis* were injected with 75 ng of a 1:1 molar ratio of cRNAs and maintained in standard oocyte saline solution: 96 mM NaCl, 2 mM KCl, 1 mM MgCl_2 , 1.8 mM CaCl_2 , 10 mM 4-(2-hydroxyethyl)-1-piperazineethanesulfonic acid (HEPES), 200 mg/L sodium pyruvate, pH 7.4, for 1–4 days at 18°C. Expression studies of $\text{Ca}_v1.1$ were performed similarly, except 100 ng of the cRNA mixture ($\text{Ca}_v1.1$, $\alpha_2\delta$, β_1 and Stac3) was injected and oocytes were stored in 0.5× Leibovitz's L-15 medium (HyClone) supplemented with 1% horse serum, 100 U/ml penicillin, 100 µg/ml streptomycin and 100 µg/ml amikacin. All experiments were performed within the guidelines established by the Institutional Animal Care and Use Committees at the University of Chicago and the University of California, Los Angeles.

Expression of $\text{hNa}_v1.4$ and $\text{h}\beta 1$ in HEK293t cells

Expression studies of $\text{hNa}_v1.4$ in mammalian cells were performed by transient transfection in HEK293t cells as previously described (Takahashi and Cannon, 1999). Briefly, plasmid cDNAs encoding wild type and mutant human $\text{Na}_v1.4$ α -subunits (0.42 µg/35-mm dish), the human Nav channel $\beta 1$ -subunit (0.42 µg/35-mm dish) and a CD8 marker (0.08 µg/35-mm dish) were transfected by calcium phosphate precipitation.

Electrophysiology

Sodium ionic currents were measured using a conventional whole-cell patch-clamp technique as described previously (Takahashi and Cannon, 1999). Briefly, at 2–3 days after transfection, the Human embryonic kidney (HEK) cells were trypsinized briefly and passaged onto 12 mm diameter round glass coverslips for electrophysiological recording. Individual transfection-positive cells were identified by labelling with anti-CD8 antibody crosslinked to microbeads. Currents were recorded with an Axopatch 200B amplified (Molecular Devices, San Jose, CA, USA). The tip of the electrode was heat-polished, and the resistance was 1.8–2.5 M Ω . Series resistance was 2–6 M Ω , and 75–80% of the series resistance was compensated by the analog circuitry of the amplifier. Cells with peak currents of <1 or >10 nA upon step depolarization from –120 mV to –10 mV were excluded. The pipette (internal) solution consisted of (mM): 105 CsF, 35 NaCl, 10 ethylene-glycol tetraacetic acid and 10 Cs-HEPES (pH 7.4). The bath solution consisted of (mM): 140 NaCl, 4 KCl, 2 CaCl₂, 1 MgCl₂, 5 glucose and 10 Na-HEPES (pH 7.4).

Charge-displacement currents and gating pore currents were recorded using a cut-open oocyte voltage clamp setup (Stefani and Bezanilla, 1998). For charge-displacement measurements, the external solution contained 115 mM *N*-methylglucamine-methylsulfonate (MS), 10 mM HEPES, and 2 mM Ca-MS, pH 7.4. The internal solution contained 115 mM *N*-methylglucamine-methylsulfonate, 10 mM HEPES and 2 mM ethylene-glycol tetraacetic acid, pH 7.4. For recording rNa_v1.4 currents, oocytes were voltage-clamped at –100 mV for at least 5 min to remove slow inactivation. After measurements of gating currents, the solution in the chambers was replaced into the pair of solutions; the external solution contained 115 mM Na-MS, 10 mM HEPES and 2 mM Ca-MS, pH 7.4 and the internal solution contained 115 mM *N*-methylglucamine-methylsulfonate, 10 mM HEPES and 2 mM ethylene-glycol tetraacetic acid, pH 7.4. To block ionic currents, 10 μ M tetrodotoxin was applied to the upper and guard chambers. After replacing solutions, the oocyte membrane was held at –100 mV, again, for at least 5 min, then the gating pore currents were recorded. For recording Ca²⁺ currents in oocytes expressing hCa_v1.1 channels, the external solution contained 96 mM Na-MS, 6 mM Ca²⁺ acetate, 10 mM HEPES, pH 7.0 with methanesulfonic acid. In some gating pore experiments, the Na-MS was reduced to 60 mM and the solution was supplemented with 60 mM guanidinium acetate. The ‘early current’ 3–4 ms after a test depolarization was measured to test for the presence of a gating pore current. This time window is after the charge-displacement current has settled, but too early for activation of the Ca²⁺ current through the pore, and thereby provides an optimal interval isolating the gating pore current (Wu et al., 2018b). Blockers were not used

to suppress the Ca²⁺ current to avoid the possibility of also blocking a gating pore current.

Data analysis

The currents from *Xenopus* oocytes were recorded with a PC44 board and digitized on the 16-bit A/D converter, and were sampled at 10 ms/point. The data acquisition program was developed in house. For gating currents measurements, linear leak and membrane capacitive currents were subtracted manually using currents obtained from a subtracting holding potential of +20 mV. All data were obtained at 20°C. Gating pore currents were obtained without any subtraction.

The ionic currents obtained from HEK293t cells were acquired by Digidata 1440A (Molecular Devices, San Jose, CA, USA) and pClamp 10 software (Molecular devices, San Jose, CA, USA) was used for the data collection. Curve fitting was manually performed using Origin software (Microcal LLC, Northampton, MA, USA) as stated previously (Takahashi and Cannon, 1999).

Statistical analysis

All data indicate the mean values \pm standard error of the mean. Statistical significance was determined in cases where *P*-values were less than 0.05 by unpaired *t*-test.

Data availability

The data which support the findings in this study are available from the corresponding authors when we receive the reasonable requests.

Results

Cases

Case I

The proband is a 16-year-old Japanese boy. One day, the patient felt muscle pains after Judo class. On the next day, the weakness in upper limbs appeared, spreading to lower limbs on the following day. On the fourth day after the judo class, the patient was brought to the emergency department because of severe weakness in all limbs. Upon arrival, he had tetraparesis with a Medical Research Council (MRC) Grade 2/5 in upper limbs and the Grade 1/5 in the lower limbs. There is no family history of neuromuscular disorders. The laboratory data showed hypokalaemia (1.5 mmol/l) and hyperCKemia (603 U/l), but no abnormality in thyroid function or adrenal function. The ECG revealed abnormal U waves and prolonged Q-Tc, most likely due to hypokalaemia. Potassium chloride was administered intravenously, with

monitoring of ECG and serum potassium. After a few days of treatment, his tetraparesis recovered completely, and he showed no neurological deficit. In order to confirm a suspected diagnosis of HypoPP, clinical neurophysiological assessment was performed. Nerve conduction study showed no abnormalities. Needle electromyography did not reveal myotonic discharges or spontaneous activity in all muscles examined including *biceps brachii*, *first dorsalis interosseus*, *vastus lateralis* and *tibialis anterior* muscles. The compound muscle action potential (CMAP) during the short exercise test showed no apparent changes (Supplementary Fig. 1). The prolonged exercise test, performed after potassium chloride administration, revealed a marked decrement of the CMAP amplitude (−30%) compared to the reference before the exercise task (Fig. 1B) (Fournier *et al.*, 2004; Tan *et al.*, 2011). Genetic analysis using the DNA extracted from the patient's and both parents' lymphocytes was performed. The proband had a heterozygous substitution (c. 2690G>A) in *CACNA1S* gene resulting in p. R897K mutation in Ca_v1.1, which was not present in either parent. The clinical, CMAP exercise, and genetic data support a diagnosis of *de novo* HypoPP type 1, with R897K missense mutation of Ca_v1.1 (Fig. 1A).

Cases 2-1 and 2-2

The probands were two French brothers. The elder brother, Case 2-1, experience repeated episodes of tetraparesis with hypokalaemia since adolescence. He developed a myopathy at age 55, at which time a muscle biopsy showed vacuoles and tubular aggregates. The patient died from liver cancer. A clinical electrophysiological assessment was never performed. The younger brother, Case 2-2, showed repeated episodes of tetraparesis since age 16. Serum potassium concentration during the paralytic attack was measured only once, which showed around 1 mmol/l. He reported 3–4 attacks per year over a period of 10 years that were triggered by rest after strenuous exercise, alcohol or carbohydrates-rich meals. The prolonged exercise test at the age of 57 showed a significant decrement of CMAP (−31%) representing the pattern V according to Fournier's classification. The frequency of the paralytic attacks decreased with the administration of acetazolamide and potassium chloride supplementation. Beginning at age 59, permanent weakness of the pelvic girdle muscle was noticed. The patient complained of limitations with running, climbing stairs and getting up from the ground. The lower-extremity MRI scan performed at age 64 showed muscle atrophy, fatty changes and the short tau inversion recovery hyperintensity in the posterior compartment of the lower leg (thigh and calve) (Fig. 1C, Supplementary Fig. 2). The genetic analysis of the two brothers showed a heterozygous R897K mutation in *CACNA1S* gene. Their father also had similar symptoms. They had four sisters who were asymptomatic and never had genetic testing.

Case 3

The proband was a French boy who presented with a first episode of tetraparesis at age 20, following a football match. The blood potassium level measured during the paralytic attack was 2 mmol/l. He experienced episodes of tetraparesis once or twice a month for about 10 years. Triggering factors were rest after sustained exercise, cold weather and carbohydrate-rich meals. Treatment with potassium chloride supplementation and potassium-sparing diuretics (spironolactone) significantly reduced the frequency of the paralytic attacks. Since the age of 46, he developed progressive permanent weakness of the pelvic girdle with difficulties climbing stairs or rising from squatting positions. A CT scan showed paravertebral and pelvic muscle atrophy with fatty infiltration (Fig. 1D). The prolonged exercise test revealed a 25% decrement of the CMAP amplitude, whereas a 40% decrement is considered diagnostic of periodic paralysis (Fournier *et al.*, 2004; Tan *et al.*, 2011). The genetic analysis showed a heterozygous R897K mutation in *CACNA1S* gene. He has three unaffected siblings who have never been genetically tested, and there is no family history of neuromuscular disorders.

Case 4

The proband was a 36-year-old Japanese male with no family history of neuromuscular disorders. Since the age of 30, he experienced transient muscle weakness in the lower limbs, twice a month on average, but never visited the clinic. At the age of 31, he was transferred to the emergency department and hospitalized because of severe tetraparesis. The laboratory data, while still weak, showed hypokalaemia (2.1 mmol/l), hyperCKemia (541 U/L), normal thyroid function and normal adrenal function. The ECG showed low amplitude T wave in aVF and III, and U waves in V2–V5, most likely due to hypokalaemia. By giving potassium chloride, the hypokalaemia normalized, followed by the recovery of tetraparesis. At age 34, the patient experienced similar attacks of severe tetraparesis again and consulted a neurologist for the diagnosis. When he was evaluated in our outpatient clinic, there were no abnormal findings in the neurological examination. The needle electromyography examination did not reveal myotonic discharges, but the prolonged exercise test elicited a large decrement of CMAP amplitude, more than 40% (Fig. 1F) (Fournier *et al.*, 2004; Tan *et al.*, 2011). The genetic analysis revealed the heterozygous substitution (c.656G>A) in the *SCN4A* gene resulting in p. R219K in Na_v1.4 (Fig. 1E). The material from other family members was not available for genetic analysis.

In addition to the specific variants identified for each of the cases above, we performed comprehensive whole-exon screening in all five patients for genes associated with familial periodic paralysis, including *SCN4A* (NM_000334.4), *CACNA1S* (NM_000069.3) and *KCNJ2* (NM_000891.2). No other variants, except for known

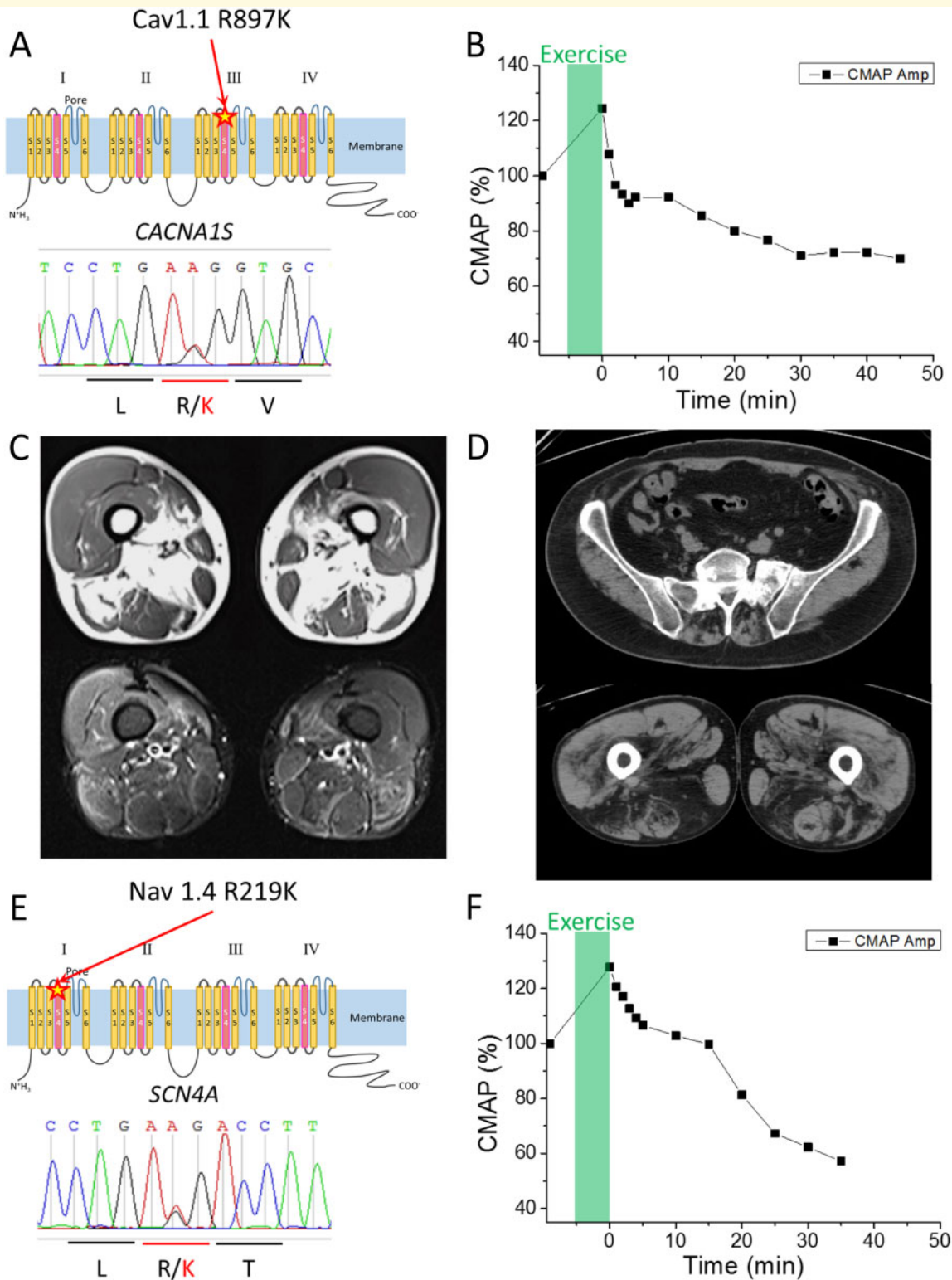


Figure 1 Clinical information of HypoPP patients with the R/K substitution in either *CACNA1S* or *SCN4A*. **(A)** Schematic representation of R897K location in Cav1.1 channel (upper panel) and the result of the Sanger sequencing obtained from Case 1. **(B)** Prolonged exercise test in Case 1 elicited an early increase and a late decrease of ~30% for the CMAP. **(C)** MRI images of skeletal muscles in Case 2-2. T1 weighted images (upper panel) and short tau inversion recovery images (lower panel) revealed fatty infiltration in *soleus* and *medial gastrocnemius* muscles. *Quadriceps*, *gracilis*, *sartorius*, *semi-membranosus* and *semi-tendinosus* muscles are grossly respected. **(D)** CT scan images of skeletal muscle in Case 3. CT scan image of lumbar portion (upper panel) showed low density area in paraspinal muscles, indicating fatty infiltration. CT scan image of thigh (lower panel) revealed low density area in bilateral hamstrings indicating fatty infiltration. **(E)** Schematic representation of the R219K location in Nav1.4 (upper panel) and the results of Sanger sequencing obtained from Case 4. **(F)** Prolonged exercise test in Case 4 revealed a decrement of the CMAP by 40%, which supports a diagnosis of periodic paralysis.

single nucleotide polymorphisms, were detected. Neither p. R219K in Na_v1.4 nor p. R897K in Ca_v1.1 has been registered in the database of Tohoku Medical Megabank Organization (ToMMO), which has genotypes of 47 000 Japanese individuals (4.7KJPN), nor in the ExAC database. PolyPhen-2 (Adzhubei *et al.*, 2010) showed that R219K in Na_v1.4 is a ‘probably damaging’ mutation with a score of 1.000, whereas R897K in Ca_v1.1 is a ‘benign’ mutation with a score of 0.013. By Mutation Taster (Schwarz *et al.*, 2010), both R219K in Na_v1.4 and R897K in Ca_v1.1 are predicted as ‘disease-causing’ mutations. Sorting Intolerant From Tolerant (SIFT) (Sim *et al.*, 2012) displayed that both R219K in Na_v1.4 and R897K in Ca_v1.1 are ‘intolerant’. Clinical information for all cases is summarized in Table 1.

Functional analysis of Na_v1.4-R219K and Ca_v1.1-R897K

Functional expression studies of ion channel mutations associated with periodic paralysis have revealed derangements in the voltage-dependent gating of Na_v1.4, and specifically for HypoPP, the presence of an anomalous gating pore current conducted through a ‘leaky’ VSD of Na_v1.4 or Ca_v1.1 HypoPP mutant channels (Sokolov *et al.*, 2007; Struyk and Cannon, 2007; Cannon, 2010, 2015; Mi *et al.*, 2014; Wu *et al.*, 2018b). The HypoPP mutations previously shown to support gating pore currents are almost all (19 of 20) missense mutations in the first or second arginine residues of S4 transmembrane segments (i.e. near the extracellular end). The charge-preserving R/K mutations reported herein are located at the first arginine of S4 in domain I of Na_v1.4 (R219K, Fig. 1E) and at the first arginine of S4 in domain III of Ca_v1.1 (R897K, Fig. 1A). We, therefore, measured Na⁺ currents to characterize the voltage-dependence of gating for Na_v1.4 WT and R219K channels and tested for the presence of anomalous gating pore currents in Na_v1.4-R219K and Ca_v1.1-R897K by measuring currents at hyperpolarized potentials in the presence of pore blockers.

Voltage-dependence of gating was not disrupted by the Na_v1.4-R219K mutation

Sodium currents were measured from HEK293t cells transiently transfected with plasmids encoding WT or R219K Na_v1.4 plus the axillary β1 subunit. Expression of WT and R219K mutant channels was comparable with Na⁺ current densities of -394.9 ± 104.0 A/F for WT ($n=7$) and -306.5 ± 68.0 A/F for R219K ($n=8$) based on the peak current at a test potential of -10 mV. The voltage-dependence of activation was indistinguishable for WT and R219K channels, as shown by the overlapping data in the conductance–voltage relation (Fig. 2A

Table 1 Clinical information summary

Case	Pedigree (race)	1 (Japanese)		2 (French)		3 (French)		4 (Japanese)	
		Sex	Male	2-1 Male	2-1 Male	2-2 Male	Male	Male	
Genetic diagnosis			R897K in CACNA1S						R219K in SCN4A
Onset			16 years old	Adolescence		20 years old			30 years old
Family history			None (<i>de novo</i>)	+(brothers and their father)		None			None
LET			+(30% decrement)	N/A		+(25% decrement)			+(43% decrement)
Serum potassium during attack			Hypokalaemia (1.5 mmol/l)	Hypokalaemia		Hypokalaemia			Hypokalaemia
Other features			HyperCKemia (603 U/l) during PP attack	Myopathy (+) (vacuoles and tubular aggregates), Died of liver cancer		Myopathy (+)			HyperCKemia (541 U/l) during PP attack

LET indicates the prolonged exercise test.

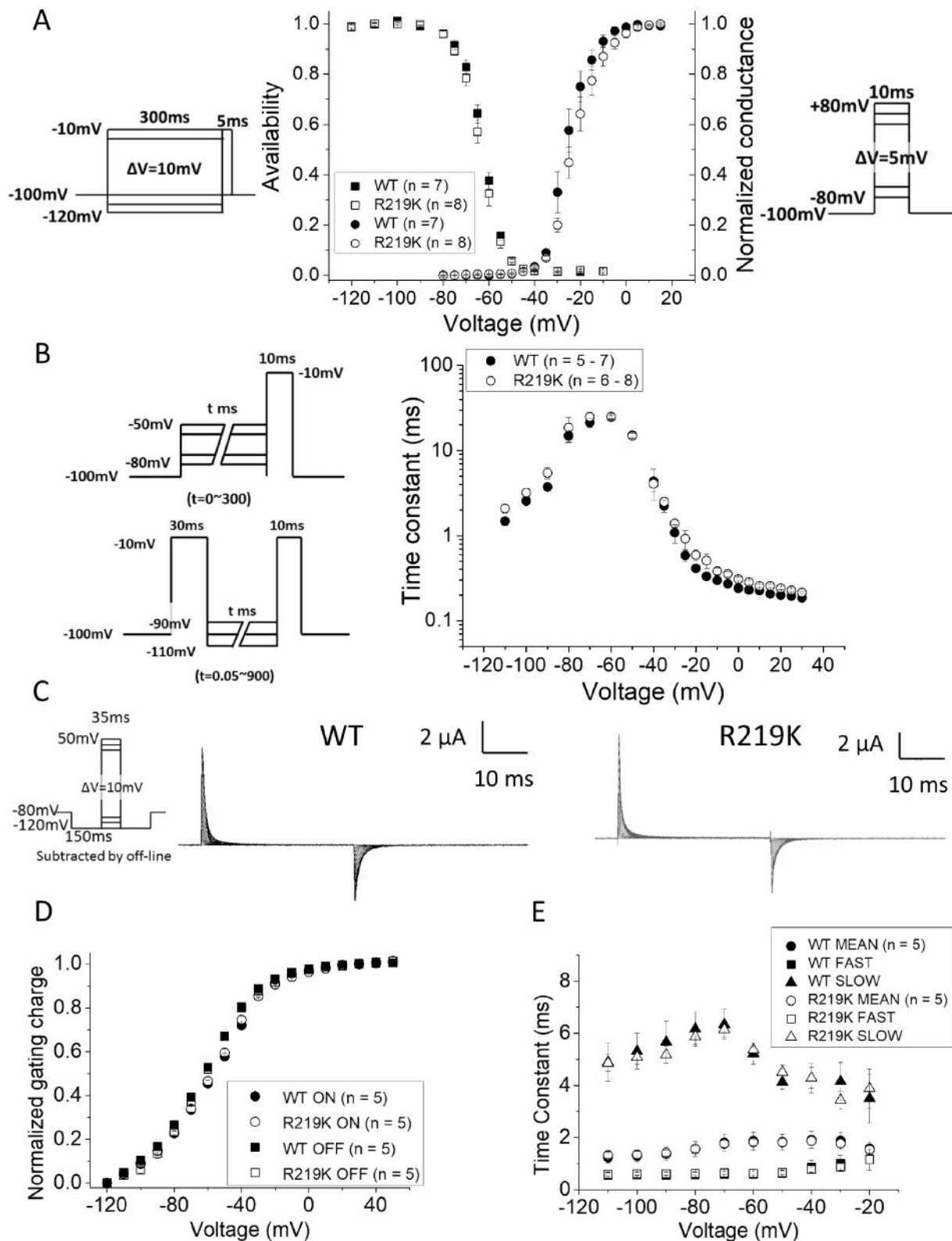


Figure 2 The functional analysis of $\text{Na}_v1.4\text{-R219K}$ gating. **(A)** The voltage dependent conductance ($G-V$ relationship) and the voltage dependent steady-state fast inactivation ($V\text{-}h_{inf}$) in wild type $\text{Na}_v1.4$ ($n = 7$) and $\text{Na}_v1.4\text{-R219K}$ ($n = 8$) are shown. The pulse protocols used are shown as insets, in the right for $G-V$ and in the left for $V\text{-}h_{inf}$. **(B)** Voltage dependent time constants for fast inactivation (Tau-V relationship) in wild type $\text{Na}_v1.4$ ($n = 5-7$) and $\text{Na}_v1.4\text{-R219K}$ ($n = 6-8$) are shown. The left upper panel indicates the two-pulse protocol for the entry to fast inactivation from -80 mV to -50 mV , and the left lower for the recovery from fast inactivation from -110 mV to -90 mV , respectively. Error bars indicate standard error of the mean. **(C)** Representative charge-displacement currents from the wild type of $\text{Na}_v1.4$ (WT) and $\text{Na}_v1.4$ with

(continued)

Table 2 Parameters for ionic Na⁺ currents in patch clamp recording fitted by two state model

	Activation		Steady-state fast inactivation	
	k (mV/e-fold)	V _{1/2} (mV)	k (mV/e-fold)	V _{1/2} (mV)
WT (n = 7)	4.2 ± 0.4	-25.5 ± 1.4	4.6 ± 0.2	62.6 ± 0.8
R219K (n = 8)	5.0 ± 0.4	-22.5 ± 1.6	4.7 ± 0.3	63.7 ± 0.9

V_{1/2} indicates the mid-point value of the steady-state fast inactivation curve (V-hinf) and the voltage dependence of activation (G-V). k is the slope factor. Errors indicate standard error of the mean.

right axis and [Supplementary Fig. 3](#)). Similarly, the inactivation gating behaviour of R219K channels was comparable to WT for steady-state voltage-dependence ([Fig. 2A](#), left axis), as were the kinetics of entry to and recovery from inactivation ([Fig. 2B](#)). All gating parameters of Na⁺ ionic currents are shown in [Table 2](#).

Movement of the channel voltage-sensor in response to a change in membrane potential was measured as the charge-displacement current in the cut-open oocyte preparation ([Fig. 2C-E](#)), where the channel expression is higher and the clamp speed is faster. The voltage for the mid-point of charge displacement, as well as the steepness with voltage, were indistinguishable for WT and R219K channels, which is consistent with the expectations for a charge-conserving mutation of the voltage-sensor domain.

Gating pore current is small for Na_v1.4-R219K and undetectable for Ca_v1.1-R897K

The oocyte expression system was used to test for the presence of anomalous gating pore currents because the sensitivity is increased by the higher membrane expression of channel density compared to HEK293t cells. The Na-conducting pore was blocked by tetrodotoxin, and steady-state currents were measured for a series of test depolarizations from a holding value of -100 mV. The current amplitude was divided by the maximal charge-displacement, to normalize for the expression level of Na_v1.4 channels in each oocyte, and plotted as a function of test potential ([Fig. 3A](#)). An excess of inward current (negative) was detected at voltages of -80 mV and more negative, for oocytes expressing Na_v1.4-R219K channels compared to WT. This difference is consistent with a gating pore current. Moreover, the inward rectification of this current shows the gating pore current is activated by hyperpolarization, which is expected for a mutation in the outermost arginine of S4 (R219K).

The inward displacement of the S4 segment with hyperpolarization brings the R219K mutation into the hydrophobic charge transfer centre, where a tight interaction with R219 normally prevents the leakage of ions. The amplitude of the R219K gating pore current, however, is much smaller than those observed in other HypoPP-2 mutant Na_v1.4 channels ([Struyk and Cannon, 2007](#); [Struyk et al., 2008](#); [Francis et al., 2011](#)).

The WT or R897K Ca_v1.1 channels were co-expressed with the α_{2δ}, β₁ and Stac3 subunits in oocytes. Membrane expression of WT channels was higher than for R897K mutant channels, based on the maximum charge displacement, 0.60 ± 0.074 nC (n = 8) and 0.29 ± 0.018 nC (n = 8), respectively. We are confident that the expression level of R897K channels was sufficient to detect a gating pore current because we had previously demonstrated robust gating pore currents for the HypoPP mutation Ca_v1.1-R528H when the maximum charge displacement was comparable (0.25 nC) ([Wu et al., 2018b](#)). In an external Na⁺ solution, the early current for oocytes expressing Ca_v1.1-R897K was not different from those expressing WT Ca_v1.1 ([Fig. 3B](#)). For many, but not all, anomalous gating pore conductances created by R/X missense mutations in S4, including Ca_v1.1-R528G ([Wu et al., 2018b](#)), the gating pore current amplitude is dramatically enhanced in the presence of external guanidinium. We, therefore, tested Ca_v1.1-R897K in 60 mM external guanidinium, but again the steady-state current was identical to that observed in WT Ca_v1.1 ([Fig. 3C](#)). We conclude that under the expression conditions used in this study, there was no detectable gating pore current for Ca_v1.1-R897K channels.

Discussion

In this study, we report five cases of HypoPP from four different pedigrees in which a charge-preserving missense mutation (R/K) in S4 of a VSD was identified in Ca_v1.1

Figure 2 Continued

R219K mutation (Na_v1.4-R219K). The pulse protocol used is shown as inset in the left. (D, E) The relative charge moved by the voltage sensors (integral of charge-displacement current) is shown as a function of test potential in the Q-V relationship (D) and Tau-V relationship (E) for WT (n = 5) and Na_v1.4-R219K (n = 5), respectively. The time constant of gating currents were fitted by two-exponential fitting and plotted both fast components and slow ones separately (opened triangles and squares). The mean of time constant was calculated by the weighted average and are shown in filled marks.

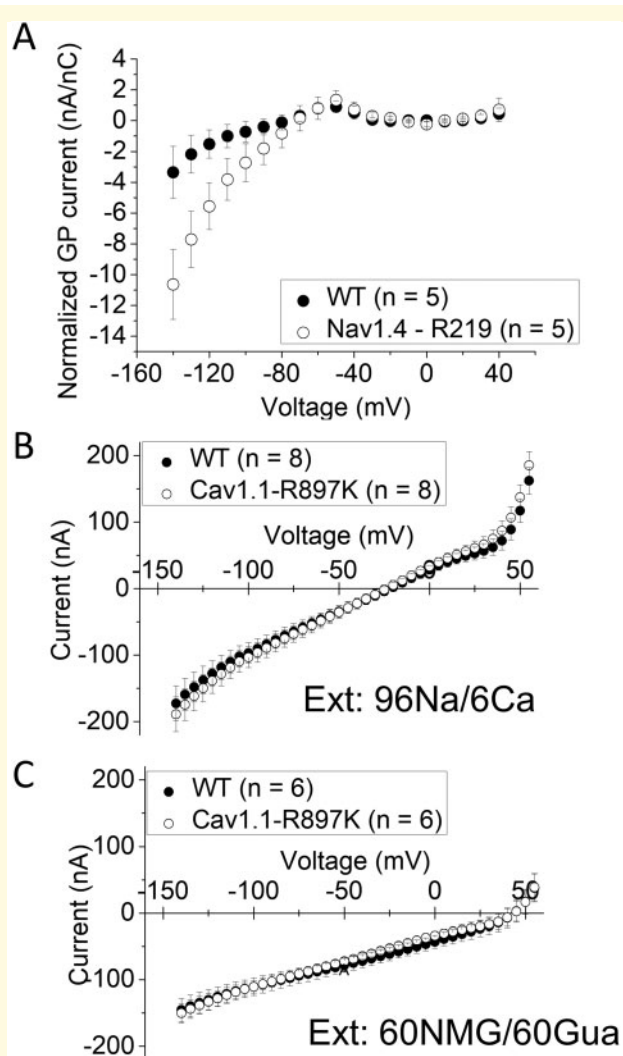


Figure 3 Gating pore current is small in $\text{Na}_V1.4\text{-R219K}$ and undetectable in $\text{Ca}_V1.1\text{-R897K}$. **(A)** Gating pore current was observed for test potentials < -80 mV ($n = 5$, respectively). Leak currents recorded were subtracted by the linear fitted line from -20 mV to $+20$ mV in each oocyte. Error bars indicate standard error of the mean. No gating pore current was detected for oocytes expression $\text{Ca}_V1.1\text{-R897K}$ in two different conditions: **(B)** external Na^+ or **(C)** a mixture of 60 mM *N*-methylglucamine and 60 mM guanidine. For **(B)**, $n = 8$ oocytes, and for **(C)**, $n = 6$ oocytes.

or $\text{Na}_V1.4$. Expression studies revealed a small gating pore current for $\text{Na}_V1.4\text{-R219K}$ channels, but no detectable gating pore current for $\text{Ca}_V1.1\text{-R897K}$ channels.

The clinical phenotypes of these R/K cases are typical for HypoPP

Recurrent episodic attacks of severe paresis with ictal hypokalaemia (<3.0 mmol/l) was observed in all five patients. Episodes were triggered by rest after exercise, ethanol or carbohydrate-rich meals, and clinical

improvement occurred with acetazolamide, K supplementation or K-sparing diuretics. Missense variants were identified in all cases, with four having $\text{Ca}_V1.1\text{-R897K}$ and one with $\text{Na}_V1.4\text{-R219K}$. These variants were not found in unaffected family members or in gene databases of subjects without neuromuscular disease. The familial transmission was demonstrated in one family with $\text{Ca}_V1.1\text{-R897K}$, and the others were *de novo*. Moreover, another missense mutation at this residue, $\text{Ca}_V1.1\text{-R897S}$, has been associated with a severe HypoPP phenotype (Chabrier et al., 2008; Hanchard et al., 2013). The prolonged CMAP exercise test was consistent with HypoPP [pattern V, with $\geq 40\%$ decrement (Fournier et al., 2004; Tan et al., 2011)] for the $\text{Na}_V1.4\text{-R219K}$ case and for one of the three $\text{Ca}_V1.1\text{-R897K}$ patients who were tested, with the other two being borderline (25–31% decrement). Among the $\text{Ca}_V1.1\text{-R897K}$ cases, 3 of 4 had clinical and imaging evidence of proximal myopathy, and in one a muscle biopsy showed vacuolar changes and T-tubular aggregates. The one case with $\text{Na}_V1.4\text{-R219K}$ did not have fixed myopathy, but he is younger than the others at age 34. Taken together, the clinical data provide convincing evidence of typical HypoPP. The genetic variants segregate with affected individuals, and all occur at arginine residues in S4 segments, adjacent to established R/X HypoPP mutations. Therefore, we propose that the $\text{Ca}_V1.1\text{-R897K}$ and $\text{Na}_V1.4\text{-R219K}$ variants are disease-causing mutations.

The anomalous gating pore current typically found for HypoPP mutant channels was not detected in the R/K mutants

The gating pore current arising from non-conserved missense mutations at the first or second arginine in the S4 segments of $\text{Ca}_V1.1$ or $\text{Na}_V1.4$ has been a consistent finding in HypoPP mutant channels. Gating pore currents are present for all 11 HypoPP R/X mutations of $\text{Na}_V1.4$ reported to date (Sokolov et al., 2007; Struyk and Cannon, 2007; Struyk et al., 2008; Francis et al., 2011; Bayless-Edwards et al., 2018). Expression studies have been performed on 7 of the 9 HypoPP mutations identified in $\text{Ca}_V1.1$. Gating pore currents were observed for six of these mutant constructs: one in a knock-in mutant mouse (Wu et al., 2012), four expressed in oocytes (Wu et al., 2018a, b) which included the same mutant construct in the knock-in mouse, and another two by transient expression in mouse skeletal muscle (Fuster et al., 2017a, b). This latter group includes the one atypical HypoPP mutation that is not located at an arginine in S4 (V876E). We did not detect a gating pore current for the HypoPP mutation $\text{Ca}_V1.1\text{-R900S}$ expressed in oocytes, but another HypoPP mutation at this same R residue caused by substitution with a smaller amino acid, $\text{Ca}_V1.1\text{-R900G}$, did support a typical gating pore current

(Wu *et al.*, 2018a). In aggregate, these multiple studies provide compelling evidence that the gating pore current is an essential contributor to the pathogenesis of HypoPP.

A gating pore current was detected for $\text{Na}_v1.4\text{-R219K}$ (Fig. 3A), but the amplitude was considerably smaller than those currents observed in other $\text{Na}_v1.4$ HypoPP mutant channels. For example, at the typical resting potential of skeletal muscle of -90 mV , the gating pore current for R219K was -2.8 nA/nC (Fig. 3A), whereas for our prior studies of HypoPP-2 mutations at R669, R672, or R1132, the gating pore current amplitude was $-48.5 \pm 13\text{ nA/nC}$ (range -17.3 to -99.7 nA/nC). A contributing factor to the small amplitude of the R219K gating pore current at -90 mV was the left-shifted (more negative) voltage for inward rectification which was about -80 mV . Similarly, we found a relatively negative rectification voltage (-45 mV) for the R669H channel, which consequently also had the smallest amplitude gating pore current (-17.3 nA/nC) amongst the HypoPP mutant channels in S4 of domain II. Both R219 and R669 are the outermost arginines in the S4 segments of domain I and II, respectively, and so a more negative membrane hyperpolarization is required to sufficiently shift the S4 segment far enough inward such that the mutant residue misaligns with the hydrophobic charge transfer centre to produce the leak. By comparison, the rectification voltage of the gating pore current for the R672 HypoPP mutant channels (second arginine from outside) is -25 mV (Struyk *et al.*, 2008).

We used our model simulation of fibre excitability (Cannon, 2018) to test whether the small-amplitude gating pore current observed for $\text{Na}_v1.4\text{-R219K}$ is sufficient to cause the paradoxical depolarization that occurs in an attack of HypoPP. Figure 4 shows the membrane potential of a simulated fibre as the extracellular K is varied. In normal muscle for which there is no gating pore current (Fig. 4, solid line in black), the membrane potential becomes more negative (hyperpolarized) as K is reduced because of the Nernst potential for K shifts to more negative potentials (e.g. 4.5 mM to 3.5 mM). In extremely low $[\text{K}^+]_o$, 2.25 mM in this example, a paradoxical depolarization to -50 mV occurs because a reduction of the inward rectifier K^+ current is no longer able to maintain the normal resting potential. At this depolarized potential, the fibre is chronically refractory and inexcitable leading to flaccid paralysis. Such low values of $[\text{K}^+]_o$ do not normally occur in vivo, and so we do not have attacks of weakness. The addition of the gating pore current, however, shifts this catastrophic depolarization to higher $[\text{K}^+]_o$ that may overlap with the low physiologic range. The question is whether the small gating pore current observed for $\text{Na}_v1.4\text{-R219K}$ is sufficient to cause susceptibility to HypoPP. As described above, the amplitude of the gating pore current at -90 mV for a typical $\text{Na}_v1.4$ HypoPP mutant channel expressed in a *Xenopus* oocyte is -48 nA/nC . This current density is equivalent to a

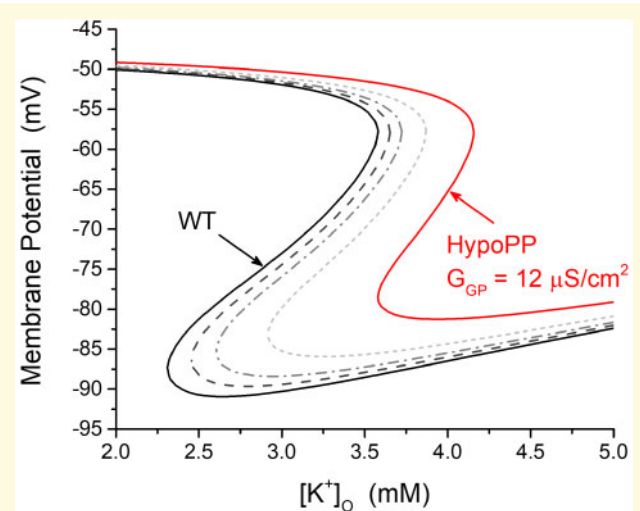


Figure 4 Simulation shows the small gating pore current for $\text{Na}_v1.4\text{-R219K}$ is not predicted to cause susceptibility to HypoPP. Curves show membrane potential as the extracellular $[\text{K}^+]_o$ is varied, for a simulated muscle fibre. Black trace indicates the response for a normal fibre, without gating pore currents. In this case, paradoxical depolarization occurs only for extremely low $[\text{K}^+]_o < 2.25\text{ mM}$. The red trace shows the response for a representative HypoPP fibre with a gating pore conductance, $G_{\text{GP}} = 12\ \mu\text{S}/\text{cm}^2$, set at the mean value observed for S4 R/X HypoPP mutant channels of domains II and III. The gating pore current causes the right shift of the curve, such that paradoxical depolarization now occurs for $[\text{K}^+]_o$ in the low physiological range (e.g. 3.5 mM). The additional curves show the response of the membrane potential if the gating pore conductance is reduced to half (short-dashed line in light grey), one-fourth (dash-dot line in grey) or one-eighth (dashed line in dark grey) of the typical value for a HypoPP mutation (solid line in red). By comparison, the gating pore current for $\text{Na}_v1.4\text{-R219K}$ at -90 mV is 17 times smaller than for other HypoPP mutant channels, which is insufficient to be a risk for HypoPP by the mechanism in this simulation.

slope conductance of $12\ \mu\text{S}/\text{cm}^2$ in a muscle fibre that is heterozygous for the HypoPP mutation, as in patients (Mi *et al.*, 2014). The addition of this gating pore leakage current now causes paradoxical depolarization in 3.5 mM $[\text{K}^+]_o$, which simulates the HypoPP phenotype (Fig. 4, solid line in red). If the amplitude of the gating pore current is reduced to 50% of the prior value, then depolarization is predicted to occur for $[\text{K}^+]_o = 2.9\text{ mM}$, a low value that rarely occurs and so an attack of HypoPP is expected to be very infrequent. If the gating pore current is further reduced to one-fourth the typical value in HypoPP, then $[\text{K}^+]_o$ must be reduced to 2.6 mM for the fibre to depolarize. Similarly, with one-eighth the gating pore current, $[\text{K}^+]_o$ must be 2.4 mM for depolarization. The gating pore current for $\text{Na}_v1.4\text{-R219K}$ at -90 mV was one-seventeenth the amplitude of a typical HypoPP mutant channel. According to our model simulations (Fig. 4), such a small leakage current is not predicted substantially shift the point of catastrophic

depolarization to a $[K^+]$ value different from normal muscle. Therefore, we conclude the small gating pore current observed for Nav1.4-R219K is not sufficient to cause a risk for HypoPP.

We were unable to detect a gating pore current for Cav1.1-R897K in the oocyte expression system. This failure is not because of limited expression of the mutant channel in the membrane because the charge-displacement current (a functional measure of voltage-sensor activity in the membrane) was comparable to the value we achieved with Cav1.1-R528H HypoPP channels that had robust gating pore currents (Wu *et al.*, 2018b). Moreover, we used a physiological extracellular solution (primarily Na^+) and did not use Cav1.1 pore blockers (e.g. Co^{2+}) that might have inadvertently blocked a gating pore conductance. Chloride-free solutions were used to greatly reduce the contribution of endogenous Cl^- currents in oocytes, which interfere with the detection of a gating pore current. The charge-conserving R/K substitution raises the interesting theoretical possibility of a Cl^- -selective gating pore leak. Although we did not test for such a possibility, a small leakage Cl^- current is not predicted to alter the excitability of a muscle fibre because the resting Cl^- conductance via ClC-1 channels is enormous. Other data clearly show that a missense mutation at Cav1.1-R897 is capable of supporting a gating pore current. The Cav1.1-R897S mutation has been identified in two *de novo* HypoPP cases, both of which had severe clinical phenotypes (Chabrier *et al.*, 2008; Hanchard *et al.*, 2013), and expression studies in oocytes revealed gating pore currents about $2\times$ larger than values observed for the most common HypoPP mutation, Cav1.1-R528H (Wu *et al.*, 2018a). Another possibility is that the oocyte expression system is inadequate to reveal the creation of an anomalous gating pore conductance for Cav1.1-R897K channels. Many potential causes could be proposed: an interacting protein is missing, post-translational modification is different in the oocyte or an endogenous substance in the oocyte occludes the gating pore conductance. Expression studies in mammalian muscle fibres are needed to explore these possibilities.

Other hypotheses for pathological mechanisms of HypoPP

In addition to the anomalous gating pore current, other functional defects of HypoPP mutant channels have been reported. For HypoPP mutations of Nav1.4 with typical clinical features, several loss-of-function defects have been reported. Inactivation (fast or slow) may be enhanced (Jurkat-Rott *et al.*, 2000; Struyk *et al.*, 2000), current density may be reduced, or the coupling of voltage-sensor movement to channel opening may be impaired (Mi *et al.*, 2014). While these loss-of-function changes would exacerbate a depolarization-induced inhibition of Na channel availability arising from the gating pore current,

these loss-of-function defects alone do not cause depolarization-induced weakness in low potassium. Because the Nav1.4-R219K variant was identified in a single proband and no genetic information is available for the parents, we cannot exclude the possibility R219K is a benign variant. If this were the case, then we propose the HypoPP phenotype may be from another gene (one-third of clinically definite HypoPP patients do not have an identified mutation in *CACNA1S* or *SCN4*) or in a non-coding region of *CACNA1S* or *SCN4A*. Atypical forms of HypoPP that are unusual because of coexisting myotonia or HyperPP have mixed gain-of-function and loss-of-function defects (Sugiura *et al.*, 2003; Kokunai *et al.*, 2018; Luo *et al.*, 2018). Alternative pathomechanisms are less apparent for HypoPP mutations of Cav1.1 without gating pore currents. The fundamental challenge is that Cav1.1 normally has little or no influence on the membrane resting potential, and so altered gating or expression level of mutant Cav1.1 is not expected to destabilize the resting potential. Two Cav1.1 mutations with convincing clinical phenotypes of typical HypoPP do not have detectable gating pore currents in the oocyte expression system: the charge-conserving Cav1.1-R897K herein and the non-conserved Cav1.1-R900S (Wu *et al.*, 2018a). These exceptions raise the possibility that another class of functional defect remains to be discovered for Cav1.1 HypoPP mutant channels.

Conclusion

This study describes five cases with typical clinical features of HypoPP, but with previously unreported charge-preserving amino acid substitutions at the outermost arginines in the voltage sensor of domain III in Cav1.1 or domain I in Nav1.4. No gating pore current was detectable for Cav1.1-R897K, and only a small gating pore current was observed for Nav1.4-R219K. Simulation studies suggest the small gating pore current for Nav1.4-R219K is not sufficient to cause paradoxical depolarization in low K^+ . These findings suggest additional functional defects, besides the gating pore leakage current, may cause susceptibility to HypoPP.

Supplementary material

Supplementary material is available at *Brain Communications* online.

Acknowledgements

All authors appreciate Dr. Francisco Bezanilla and Dr. Ana M. Correa for kind equipment support of cut-open voltage clamp set-up and providing the rNav1.4 clone and rNav β 1

clone. We thank Ms. Kimie Hayashi for her technical supports.

Funding

This work is supported by Japan Society for the Promotion of Science (JSPS) KAKENHI (JP18K07524) and by Takeda Science Foundation Grant for medical science research to T.K., by the Research Grant for Intractable Disease from the Ministry of Health, Labour and Welfare (H29-Nanchitou(Nan)-Ippan-030 and 20FC1036), the Japan Agency for Medical Research and Development (JP19ek0109230 and JP19bm0804005) and JSPS KAKENHI (JP15K09314) to M.P.T., by grants from the Institut national de la santé et de la recherche médicale (INSERM), Sorbonne University and the French Muscular Dystrophy Association (AFM-Telethon) (strategic grant to B.F.). Support was provided by National Institute of Arthritis and Musculoskeletal and Skin Diseases (NIAMS) of the National Institutes of Health (AR063182 to S.C.C.).

Competing interests

The authors report no competing interests.

References

- Adzhubei IA, Schmidt S, Peshkin L, Ramensky VE, Gerasimova A, Bork P, et al. A method and server for predicting damaging missense mutations. *Nat Methods* 2010; 7: 248–9.
- Bayless-Edwards L, Winston V, Lehmann-Horn F, Arinze P, Groome JR, Jurkat-Rott K. Nav1.4 DI-S4 periodic paralysis mutation R222W enhances inactivation and promotes leak current to attenuate action potentials and depolarize muscle fibers. *Sci Rep* 2018; 8: 10372.
- Cannon SC. Voltage-sensor mutations in channelopathies of skeletal muscle. *J Physiol* 2010; 588: 1887–95.
- Cannon SC. Channelopathies of skeletal muscle excitability. *Compr Physiol* 2015; 5: 761–90.
- Cannon SC. Sodium channelopathies of skeletal muscle. *Handb Exp Pharmacol* 2018; 246: 309–30.
- Chabrier S, Monnier N, Lunardi J. Early onset of hypokalaemic periodic paralysis caused by a novel mutation of the CACNA1S gene. *J Med Genet* 2008; 45: 686–8.
- Fournier E, Arzel M, Sternberg D, Vicart S, Laforet P, Eymard B, et al. Electromyography guides toward subgroups of mutations in muscle channelopathies. *Ann Neurol* 2004; 56: 650–61.
- Francis DG, Rybalchenko V, Struyk A, Cannon SC. Leaky sodium channels from voltage sensor mutations in periodic paralysis, but not paramyotonia. *Neurology* 2011; 76: 1635–41.
- Fuster C, Perrot J, Berthier C, Jacquemond V, Allard B. Elevated resting H⁺ current in the R1239H type 1 hypokalaemic periodic paralysis mutated Ca²⁺ channel. *J Physiol* 2017a; 595: 6417–28.
- Fuster C, Perrot J, Berthier C, Jacquemond V, Charnet P, Allard B. Na leak with gating pore properties in hypokalaemic periodic paralysis V876E mutant muscle Ca channel. *J Gen Physiol* 2017b; 149: 1139–48.
- Hanchard NA, Murdock DR, Magoulas PL, Bainbridge M, Muzny D, Wu YQ, et al. Exploring the utility of whole-exome sequencing as a diagnostic tool in a child with atypical episodic muscle weakness. *Clin Genet* 2013; 83: 457–61.
- Jurkat-Rott K, Mitrovic N, Hang C, Kouzmenkine A, Iaizzo P, Herzog J, et al. Voltage-sensor sodium channel mutations cause hypokalaemic periodic paralysis type 2 by enhanced inactivation and reduced current. *Proc Natl Acad Sci USA* 2000; 97: 9549–54.
- Kokunai Y, Dalle C, Vicart S, Sternberg D, Pouliot V, Bendahhou S, et al. A204E mutation in Nav1.4 DIS3 exerts gain- and loss-of-function effects that lead to periodic paralysis combining hyper- with hypo-kalaemic signs. *Sci Rep* 2018; 8: 16681.
- Liman ER, Tytgat J, Hess P. Subunit stoichiometry of a mammalian K⁺ channel determined by construction of multimeric cDNAs. *Neuron* 1992; 9: 861–71.
- Luo S, Sampedro Castañeda M, Matthews E, Sud R, Hanna MG, Sun J, et al. Hypokalaemic periodic paralysis and myotonia in a patient with homozygous mutation p.R1451L in Nav1.4. *Sci Rep* 2018; 8: 9714.
- Matthews E, Labrum R, Sweeney MG, Sud R, Haworth A, Chinnery PF, et al. Voltage sensor charge loss accounts for most cases of hypokalaemic periodic paralysis. *Neurology* 2009; 72: 1544–7.
- Mi W, Rybalchenko V, Cannon SC. Disrupted coupling of gating charge displacement to Na⁺ current activation for DIIS4 mutations in hypokalaemic periodic paralysis. *J Gen Physiol* 2014; 144: 137–45.
- Pan X, Li Z, Zhou Q, Shen H, Wu K, Huang X, et al. Structure of the human voltage-gated sodium channel Nav1.4 in complex with $\beta 1$. *Science* 2018; 362: eaau2486.
- Sampedro Castañeda M, Zanoteli E, Scalco RS, Scaramuzzi V, Marques Caldas V, Conti Reed U, et al. A novel ATP1A2 mutation in a patient with hypokalaemic periodic paralysis and CNS symptoms. *Brain* 2018; 141: 3308–18.
- Schwarz JM, Rödelserperger C, Schuelke M, Seelow D. MutationTaster evaluates disease-causing potential of sequence alterations. *Nat Methods* 2010; 7: 575–6.
- Sim N-L, Kumar P, Hu J, Henikoff S, Schneider G, Ng PC. SIFT web server: predicting effects of amino acid substitutions on proteins. *Nucleic Acids Res* 2012; 40: W452–W457.
- Sokolov S, Scheuer T, Catterall WA. Gating pore current in an inherited ion channelopathy. *Nature* 2007; 446: 76–8.
- Starace DM, Bezanilla F. A proton pore in a potassium channel voltage sensor reveals a focused electric field. *Nature* 2004; 427: 548–53.
- Stefani E, Bezanilla F. Cut-open oocyte voltage-clamp technique. *Methods Enzymol* 1998; 293: 300–18.
- Struyk AF, Cannon SC. A Na⁺ channel mutation linked to hypokalaemic periodic paralysis exposes a proton-selective gating pore. *J Gen Physiol* 2007; 130: 11–20.
- Struyk AF, Markin VS, Francis D, Cannon SC. Gating pore currents in DIIS4 mutations of Nav1.4 associated with periodic paralysis: saturation of ion flux and implications for disease pathogenesis. *J Gen Physiol* 2008; 132: 447–64.
- Struyk AF, Scoggan KA, Bulman DE, Cannon SC. The human skeletal muscle Na channel mutation R669H associated with hypokalaemic periodic paralysis enhances slow inactivation. *J Neurosci* 2000; 20: 8610–7.
- Sugiura Y, Makita N, Li L, Noble PJ, Kimura J, Kumagai Y, et al. Cold induces shifts of voltage dependence in mutant SCN4A, causing hypokalaemic periodic paralysis. *Neurology* 2003; 61: 914–8.
- Takahashi MP, Cannon SC. Enhanced slow inactivation by V445M: a sodium channel mutation associated with myotonia. *Biophys J* 1999; 76: 861–8.
- Tan SV, Matthews E, Barber M, Burge JA, Rajakulendran S, Fialho D, et al. Refined exercise testing can aid DNA-based diagnosis in muscle channelopathies. *Ann Neurol* 2011; 69: 328–40.
- Tao X, Lee A, Limapichat W, Dougherty DA, MacKinnon R. A gating charge transfer center in voltage sensors. *Science* 2010; 328: 67–73.
- Venance SL, Cannon SC, Fialho D, Fontaine B, Hanna MG, Ptacek LJ, et al. The primary periodic paralyses: diagnosis, pathogenesis and treatment. *Brain* 2006; 129: 8–17.

Wu F, Mi W, Burns DK, Fu Y, Gray HF, Struyk AF, et al. A sodium channel knockin mutant (Nav1.4-R669H) mouse model of hypokalemic periodic paralysis. *J Clin Invest* 2011; 121: 4082–94.

Wu F, Mi W, Hernández-Ochoa EO, Burns DK, Fu Y, Gray HF, et al. A calcium channel mutant mouse model of hypokalemic periodic paralysis. *J Clin Invest* 2012; 122: 4580–91.

Wu F, Quinonez M, Cannon SC. Gating Pore Currents in DIII Hypopp Mutations of Ca V 1.1 (Conference abstract). *Biophys J* 2018a; 114: 639a.

Wu F, Quinonez M, DiFranco M, Cannon SC. Stac3 enhances expression of human CaV1.1 in *Xenopus* oocytes and reveals gating pore currents in HypoPP mutant channels. *J Gen Physiol* 2018b; 150: 475–89.